

Finite Element Analysis of Spring-back Characteristics on Asymmetrical Z-shape Parts in Wiping Z-bending Process

Wiriyakorn Phanitwong, Pakkawat Komolruji and Sutasn Thipprakmas
*Dept. of Tool and Materials Engineering, King Mongkut's University of Technology Thonburi,
PrachaUthit Rd., Bangkok, Thailand*

Keywords: Z-bending Process, Wiping-bending Process, Z-shape, Spring-back, Asymmetry, Finite Element Method.

Abstract: In recent years, the Z-bending process was rarely investigated, especially for the asymmetrical Z-shape bending process. This causes the lacks of understanding on bending mechanism and spring-back characteristics and results in the difficulty in die design and process control for the spring-back characteristics. In the present research, therefore, the wiping asymmetrical Z-bending process was examined by using the finite element method (FEM) and laboratory experiments. On the basis of the stress distribution analysis, the different of spring-back characteristics between the symmetrical and asymmetrical wiping Z-bending processes were investigated and clearly identified. In addition, the effects of working process parameters, including bend angle and tool radius on spring-back characteristics were investigated and clearly identified via the changes of stress distribution analysis as well. To verify the accuracy of the FEM-simulation results, the laboratory experiments were carried out. The experiments were carried out to validate the FEM simulation results. The FEM simulation results showed a good agreement with the experimental results with reference to the bend angles.

1 INTRODUCTION

A sheet-metal bending process being a common forming process is widely employed to form curved shapes in sheet-metal parts by using a die. The bending die could be commonly classified on the basis of its design shape, including L-, V-, U-, or Z-bent shaped parts (Lange, 1985; Schuler, 1998). In the past, most researches of bending process were carried out to investigate for fabrication of L-, V-, and U-bent shaped parts. Many previous researches are aimed to assess product quality upgrades as well as to assess precise prediction of the spring-back characteristic (Dilip Kumar, 2014; Zong, 2014, Phanitwong, 2014; Leu, 2015; Thipprakmas, 2015). With the fabrication of Z-bent shape parts, in the past, they were usually designed to perform by two bending operations though V-bending processes. Therefore, the theory of Z-bending process is based on the theory of V-bending processes. For these reasons, they resulted in a lack of research on the Z-bending process. However, in terms of low-cost manufacturing, the strategies against low-cost competition have been entirely considered in recent years. To satisfy this low-cost manufacturing, the

wiping Z-bending process, which uses the Z-shape die and can make two bends though one stroke on a press machine as depicted in Fig. 1, has been proposed to reduce the number of bending operations and production time. Although the principle of wiping Z-bending process is similar to wiping-bending or L-bending process, the bending mechanisms of them are different (Komolruji, 2013). For these reasons, the previous researches on L-bending process (Dilip Kumar, 2014; Kuo, 2012) could not be applied for the wiping Z-bending process. In addition, in recent years, the complicated Z-shape parts with the high precision such as asymmetrical Z-shape parts are increasingly required. Therefore, the lack of research on wiping Z-bending process means that a basic database with its information is insufficient to design a suitable bending die to control the spring-back characteristics. Therefore, understanding the bending mechanism and spring-back characteristics is necessary. In the present research, therefore, the asymmetrical Z-shape parts was investigated though the wiping Z-bending process using FEM and laboratory experiments. On the basis of the stress distribution analyses, the different of spring-back

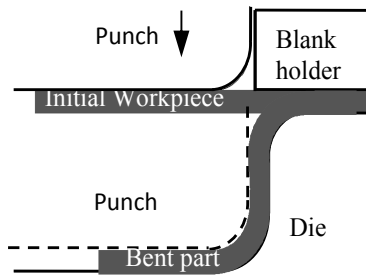


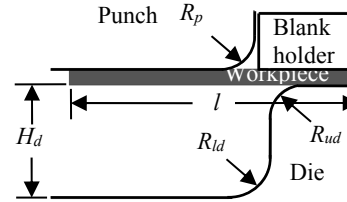
Figure 1: Principle of wiping Z-bending process.

characteristics between the symmetrical and asymmetrical wiping Z-bending processes was investigated and clearly identified by analyzing the changes in the stress distribution. In addition, the effects of working process parameters, including bend angle and tool radius on the spring-back characteristics were investigated and clearly identified by analyzing the changes in the stress distribution as well. To verify the accuracy of the FEM simulation results, laboratory experiments were performed. The FEM simulation results showed good agreement with the experimental results in terms of the bend angles.

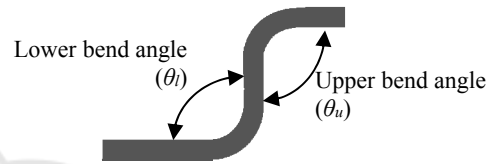
2 THE FEM SIMULATION AND EXPERIMENTAL PROCEDURES

In the present study, Fig. 2(a) shows the model of the wiping Z-bending process which was investigated. Fig. 2(b) depicted the measured bend angles in the Z-shape parts. The details of these models and the process parameter conditions investigated in the present research were listed in Table 1. Specifically, the three asymmetrical bend angle and tool radius levels, as listed in Table 1, were investigated. A two-dimensional plane strain with a thickness of 3 mm was applied. The two-dimensional, implicit, quasi-static finite element method of a commercial analytical code, DEFORM-2D, was used for the FEM simulation. To prevent the excessive deformation of the elements, the adaptive remeshing function was applied. As per past studies (Komolruji, 2013; Phanitwong, 2014), the punch and die were set as rigid types and the workpiece material was set as an elasto-plastic type. The rectangular elements approximately 4,000 elements were generated on workpiece material. To save the calculation time, this number of element is the least number to assess precise prediction of the spring-back characteristic. The workpiece material

used in the present study was aluminum A1100-O (JIS) and its properties were taken from tensile test data. The strength coefficient and the strain hardening exponent values were 153.5 MPa and 0.20, respectively.



(a) FEM simulation model



(b) Measured bend angles

Figure 2: FEM simulation model and measured bend angles.

Table 1: FEM simulation and experimental conditions.

Simulation model	Plane strain model
Object types	Workpiece : Elasto-plastic Punch/Die : Rigid Blank holder : Rigid
Workpiece material	A1100-O, Thickness (t): 3 mm
Flow curve equation	$\bar{\sigma} = 153.5\bar{\epsilon}^{0.20} + 88$
Friction coefficient (μ)	0.1
Workpiece length (l)	60 mm
Web height (H_d)	20 mm
Punch radius (R_p)	3, 5, 7 mm
Upper bend radius (R_{ud})	3 mm
Lower bend radius (R_{ld})	6, 8, 10 mm
Upper bend angle (θ_u)	90°
Lower bend angle (θ_l)	90°, 120°, 150°

Next, laboratory experiments were performed to validate the FEM simulation results. As per experiments from past researches (Komolruji, 2013, Phanitwong, 2014), a 5-ton universal tensile testing machine (Lloyd Instruments Ltd.) was used as the press machine. Fig. 3 shows the wiping Z-die used for the experiments. Five samples from each bending condition were used to inspect the obtained bend angles. After unloading a profile projector

(Mitutoyo model PJ-A3000) was used for the bend angle measurement. The observed bend angle and bending force were recorded and compared with those analyzed by the FEM simulation.

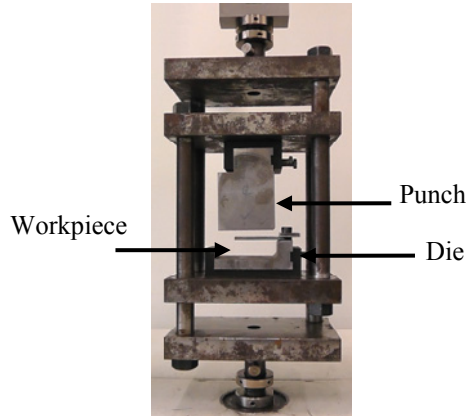


Figure 3: The punch and die components for experiments.

3 RESULTS AND DISCUSSIONS

3.1 Asymmetrical Bend Radius

Fig. 4 shows the comparison of stress distribution analyses before unloading phase between symmetrical and asymmetrical bend radius cases. Fig. 4(a) and (b) show the symmetrical and asymmetrical bend radius cases, respectively. First, the manners of the stress distribution analysis corresponded well with the bending theory and the literature (Komolruji, 2013). Specifically, the stress distribution not only generated in bending allowance zone as depicted in zone A and zone B, but it also generated in the web as depicted in zone C as well as generated in leg as depicted in zone D. Next, as the lower bend radius increased as shown in Fig. 4(b), the bending allowance zone increased as well as stress distribution increased as depicted in zone B. This manner of the stress distribution analysis again corresponded well with the bending theory and the literature (Lange, 1985; Schuler, 1998; Thipprakmas, 2011). In addition, as shown in Fig. 4(b), the increase in lower bend radius resulted in the decrease in stress distribution the web as depicted in zone C as well as resulted in the increase in the stress distribution in the leg as depicted in zone D. Fig. 5 shows the comparison of predicted bend angles after unloading. As illustrated in Fig. 5(a), in the case of symmetrical bend radius, the predicted upper bend angle (θ_u) and lower bend angle (θ_l) were of 90.31° and 88.83° , respectively.

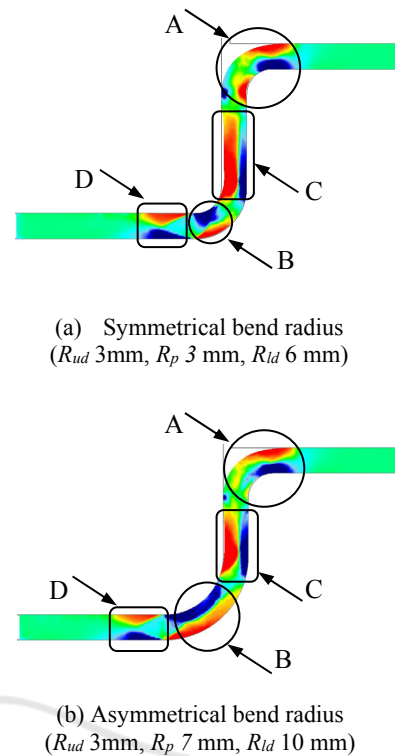


Figure 4: Illustration of stress distribution analysis before unloading with respect to the lower bend radius (θ_u 90° , θ_l 90°).

Next, in the case of asymmetrical bend radius as shown in Fig. 5(b), the predicted upper bend angle (θ_u) and lower bend angle (θ_l) were of 90.92° and 85.59° , respectively. In terms of predicted lower bend angle, the results illustrated that the predicted lower bend angle (θ_l) increased as the lower bend radius increased. Specifically, the amount of spring-back increased as the lower bend radius increased. This manner of the spring-back characteristic corresponded well with the bending theory and the literature (Lange, 1985, Schuler, 1998, Thipprakmas, 2011).

In addition, the results also illustrated that the predicted upper bend angle was changed as the lower bend radius increased. As these results, they confirmed that the change in bend radius on one side resulted in the change in spring-back characteristic on the opposite side. The effects of lower bend radius on spring-back characteristics were also examined. Fig. 6 shows effects of lower bend radius on spring-back characteristics in upper and lower bend angles. As abovementioned, as the lower bend

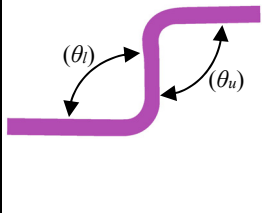
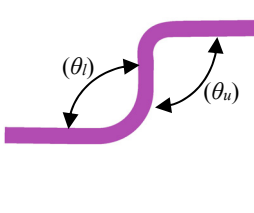
(a) Symmetrical case (R_{ud} 3mm, R_p 3 mm)	(b) Asymmetrical case (R_{ud} 3mm, R_p 7 mm)
	
θ_u 90.31° and θ_l 88.83°	θ_u 90.92° and θ_l 89.59°

Figure 5: Comparison of predicted bend angles after unloading between symmetrical and asymmetrical bend radius (θ_u 90°, θ_l 90°). (Komolruji, 2013).

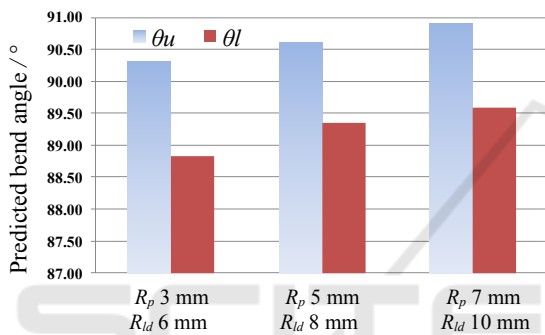


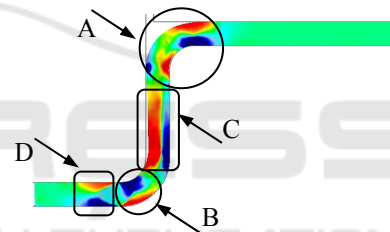
Figure 6: Relationship between lower bend radius and the predicted bend angles (R_{ud} 3 mm, θ_u 90°, θ_l 90°). (Komolruji, 2013).

radius increased, it caused the increases in stress distribution in bending allowance zone (zone B) and in leg (zone D) as well as the decrease in stress distribution in web (zone C). After compensating these changes in stress distributions, as per the previous research (Komolruji, 2013), the results elucidated that as the lower bend radius were 3 mm, 5 mm, and 7 mm, the predicted upper and lower bend angles were 90.31° and 88.83°, 90.62° and 89.35°, 90.92° and 89.59°, respectively. As these results, the results confirmed that as the lower bend radius increased the amount of spring-back in the upper bend angle increased as well as the amount of spring-back in the lower bend angle increased.

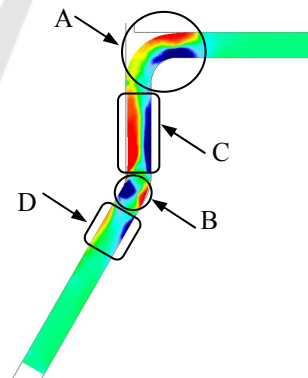
3.2 Asymmetrical Bend Angle

Fig. 7 shows the comparison of stress distribution analyses before unloading phase between symmetrical and asymmetrical bend angle cases. Fig. 7(a) and (b) show the symmetrical and asymmetrical bend angle cases, respectively. As the

lower bend angle increased, the bending allowance zone decreased as well as stress distribution decreased as depicted in zone B. This manner of the stress distribution analysis again corresponded well with the bending theory and the literature (Lange, resulted in the decrease in the stress distribution in the leg as depicted in zone D. Fig. 8 shows the comparison of predicted bend angles after unloading. As illustrated in Fig. 8(a), in the case of 1985, Schuler, 1998, Thipprakmas, 2011). In addition, as shown in Fig. 7(b), the increase in lower bend angle resulted in the decrease in stress distribution the web as depicted in zone C as well as symmetrical bend angle, the predicted upper bend angle (θ_u) and lower bend angle (θ_l) were of 90.31° and 88.83°, respectively. Next, in the case of asymmetrical bend angle as shown in Fig. 8(b), the predicted upper bend angle (θ_u) and lower bend angle (θ_l) were of 91.64° and 149.30°, respectively. In terms of predicted lower bend angle, the results illustrated that the amount of spring-back decreased as the lower bend angle increased.



(a) Symmetrical bend angle (θ_u 90°, θ_l 90°)



(b) Asymmetrical bend angle (θ_u 90°, θ_l 150°)



Figure 7: Illustration of stress distribution analysis before unloading with respect to the lower bend angle. (R_{ud} 3mm, R_{ld} 6 mm, R_p 3 mm).

(a) Symmetrical case (θ_u 90°, θ_l 90°)	(b) Asymmetrical case (θ_u 90°, θ_l 150°)
θ_u 90.31° and θ_l 88.83°	θ_u 91.64° and θ_l 149.30°

Figure 8: Comparison of predicted bend angles after unloading between symmetrical and asymmetrical bend angle. (R_{ud} 3mm, R_{ld} 6 mm, R_p 3 mm).

This manner of the spring-back characteristic corresponded well with the bending theory and the literature (Lange, 1985, Schuler, 1998, Thipprakmas, 2011). In addition, the results also illustrated that the predicted upper bend angle was changed as the lower bend angle increased. As these results, they confirmed that the change in bend angle on one side resulted in the change in spring-back characteristic on the opposite side. The effects of lower bend angle on spring-back characteristics were also examined. Fig. 9 shows effects of lower bend angle on spring-back characteristics in predicted upper and lower bend angles. As abovementioned, as the lower bend angle increased, it caused the decreases in stress distribution in bending allowance zone (zone B) and in leg (zone D) as well as the decreases in stress distribution in web (zone C). After compensating these changes in stress distributions, the results elucidated that as the lower bend angle were 90°, 120°, and 150°, the

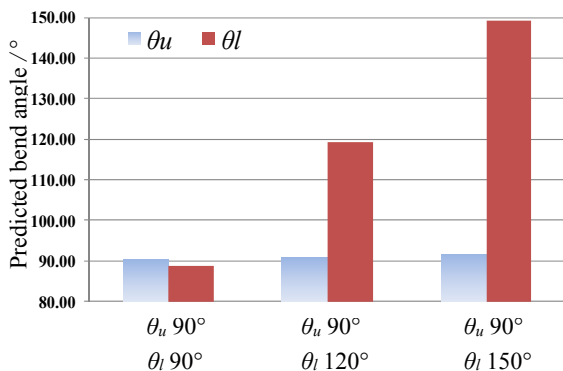


Figure 9: Relationship between lower bend angle and the predicted bend angles. (R_{ud} 3mm, R_{ld} 6 mm, R_p 3 mm).

predicted upper and lower bend angles were 90.31° and 88.83°, 90.92° and 119.35°, 91.64° and 149.30°, respectively. As these results, the results confirmed that as the lower bend angle increased the amount of spring-back in the upper bend angle increased as well as the amount of spring-back in the lower bend angle increased.

3.3 Validation of FEM Simulation Results

In this research, to validate the accuracy of the FEM simulation results, the laboratory experiments were carried out. Fig. 10 shows the comparison of the bend angle between the FEM simulation and experimental results. As per the past research (Komolruji, 2013), the FEM simulation result showed good agreement with the experimental result, in which the error in the bend angle as compared to the experimental result was approximately 1 %.

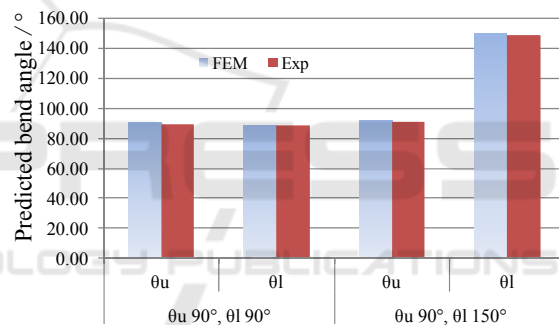


Figure 10: Comparison of the predicted bend angle between the FEM simulation and experimental results. (R_{ud} 3mm, R_{ld} 6 mm, R_p 3 mm).

4 CONCLUSIONS

In the present research, to study the spring-back characteristic on asymmetrical Z-shape parts in wiping Z-bending process, the FEM simulation was used to identify the effects of working process parameters, including bend radius and bend angle, on the spring-back characteristic. Based on the stress distribution analysis, the bending mechanism of asymmetrical Z-shape and the spring-back characteristic were clearly identified comparing with those in the symmetrical Z-shape case. The results illustrated that the change in bend radius or bend angle on one side resulted in the change in spring-back characteristic on its side and on the opposite side as well. The effects of bend radius and bend

angle on spring-back characteristics were also examined by analyzing the changes in the stress distribution. In terms of bend radius, the amount of spring-back in the lower bend angle increased as the lower bend radius increased. In addition, it also caused in the change in upper bend angle, in which the amount of spring-back in the upper bend angle increased as the lower bend radius increased. Next, In terms of bend angle, the amount of spring-back in the lower bend angle increased. Again, this also caused in the change in upper bend angle, in which the amount of spring-back in the upper bend angle increased as the lower bend angle increased. The FEM simulation results, as validated by laboratory experiments, showed that the errors in the bend angle compared with the laboratory experimental results were approximately 1 %.

ACKNOWLEDGEMENTS

The authors would like to express their gratitude to the National Research University Project of Thailand, Office of the Higher Education Commission, under Grant No. 57000618 for their financial assistance to this study. The authors also thank Mr. Arkarapon Sontamino, graduate students, for their help in this study.

REFERENCES

- Dilip Kumar, K., Appukuttan, K. K., Neelakantha, V. L., Naik, P. S., 2014, Experimental determination of spring back and thinning effect of aluminum sheet metal during L-bending operation, *J Mater Des*, 56: 613–619.
- Komolruji, P., Thipprakmas, S., 2013, Finite Element Analysis of Bending Angle Precision in Z-bending Process, *International Conference on Materials Processing Technology (Proc. of MAPT2013)*, p. 41.
- Kuo, C. C., Lin, B. T., 2012, Optimization of springback for AZ31 magnesium alloy sheets in the L-bending process based on the Taguchi method, *Int. J. Adv. Manuf. Technol*, 58:161–173.
- Lange, K., 1985, *Handbook of metal forming*. McGraw-Hill Inc., New York.
- Leu, D. K., 2015, Position deviation and springback in V-die bending process with asymmetric dies, *Int J Adv Manuf Technol*, 79:1095–1108.
- Phanitwong, W., Thipprakmas, S., 2014, Determination of coined bead geometry in the V-bending process, *Adv Mech Eng*, 6:345152.
- Schuler, 1998, *Metal forming handbook*. Springer, Berlin.
- Thipprakmas, S., Boochakul, U., 2015, Comparison of spring-back characteristics in symmetrical and asymmetrical U-bending processes, *Int J Precis Eng Manuf*, 16(7):1441–1446.
- Thipprakmas, S., Phanitwong, W., 2011, Process parameter design of spring-back and spring-go in V-bending process using Taguchi technique, *J Mater Des*, 32 (8-9):4430-4436.
- Zong, Y.Y., Liu, P., Guo, B., Shan, D., 2015, Springback evaluation in hot V-bending of Ti-6Al-4V alloy sheets. *Int J Adv Manuf Technol*, 76:577–585.